UAB
Universitat Autònoma de Barcelona

Dipòsit digital de documents de la UAB

This is the **published version** of the master thesis:

Román, Elena Ortiz de Zárate; Rodríguez Álvarez, José , dir.; Miñano Molina, Alfredo Jesús. Synaptic dysfunction induced by A oligomers in Alzheimer's disease: AKAP150–NFAT signalling as a molecular target. 2025. 31 pag. (Màster Universitari en Bioquímica, Biologia Molecular i Biomedicina)

This version is available at https://ddd.uab.cat/record/320136

under the terms of the CC BY-SA license

Masters in Biochemistry, Molecular Biology and Biomedicine final project

Synaptic dysfunction induced by Aβ oligomers in Alzheimer's disease: AKAP150–NFAT signalling as a molecular target

Author: Elena Ortiz de Zárate Román

Tutors: José Rodríguez Álvarez and Alfredo Jesús Miñano Molina

Institut de Neurociències Departament de Bioquímica i Biología Molecular

Unitat de Bioquímica, Facultat de Medicina

Universitat Autònoma de Barcelona

To my family, especially Aihen.

To my friends back home, my reynas, Irati and Garazi.

To the friends that came with me, Maialen and Irati.

To the new friends I made here, from the master's and the lab.

And to myself.

ABSTRACT

Alzheimer's disease (AD) is the most common form of dementia worldwide and to this day no effective cure has been found. Various studies suggest that synaptic dysfunction is one of the earliest pathological events in this disease, preceding even clinical symptoms. In this regard, soluble amyloid-beta oligomers (Aβo) have been identified as neurotoxic compounds that can alter synaptic function. The aim of this study is to investigate the molecular effects of Aβo on some key components of the postsynaptic signalling complex in hippocampal neuronal cultures, focusing on the AKAP-CaN-NFAT signalling pathway, which includes scaffolding protein AKAP79/150, phosphatase calcineurin (CaN) and transcription factor NFATc3. In this research, we observed that Aβo reduce the expression of AKAP150 in a time-dependent manner. This reduction was not prevented by the blocking of L-type calcium channels (LTCCs), suggesting that LTCCs are not involved in Aβo-induced AKAP150 decrease. Additionally, Aβo alter the cellular localization of NFATc3 and modify dendritic distribution. Collectively, these results suggest that Aβo trigger time-dependent dynamic alterations in the AKAP-CaN-NFAT complex, potentially disrupting postsynaptic organization and affecting gene-expression. Our findings support the understanding of early molecular mechanisms that contribute to synaptic dysfunction in AD and open the possibility of identifying these compounds as therapeutical targets.

LIST OF ABBREVIATIONS

Aβ	Amyloid-beta
Aβo	Amyloid-beta oligomers
ACSF	Artificial cerebrospinal fluid
AD	Alzheimer's disease
AMPA	α-amino-3-hydroxy-5-methyl-4-isoxazolepropionic acid receptors
AKAP79/150	A-kinase anchoring protein 79/150
BSA	Bovine serum albumin
CaMKII	Ca2+/calmodulin kinase II
CSF	Cerebrospinal fluid
DIV	Days in-vitro
DMEM	Dulbecco's modified Eagle's medium
DMSO	Dimethyl sulfoxide
FUDR	Fluoro deoxyuridine
GAPDH	Glyceraldehyde-3-phosphate dehydrogenase
HRP	Horseradish peroxidaseconjugated
LTD	Long-term depression
LTP	Long-term potentiation
NFAT	Nuclear factor of activated T-cells
PBS	Phosphate-buffered saline
PDL	Poly-D-lysine
PFA	Paraformaldehyde
PKA	Protein kinase A
PKC	Protein kinase C
pNFAT	Phosphorylated nuclear factor of activated T-cells
NIMO	Nimodipine
NMDA	N-methyl-D-aspartate receptors
PSD-95	Postsynaptic density protein 95

CONTENT

INTRODUCTION **7**
1. Alzheimer's disease 7
1.1 Alzheimer's overview 7
1.2 Neuropathology of the disease 7
1.3 Diagnostic and treatment for Alzheimer's disease 8
2. Synaptic plasticity alterations in Alzheimer's disease 9
2.1 Synaptic plasticity and physiological significance 9
2.2 Molecular mechanisms of LTP and LTD 10
2.3 Oligomeric Aβ-induced synaptic dysfunction 10
3. Dysregulation of post-synaptic signalling complexes by Aβo 11
3.1 AKAP79/150 as an integrator of synaptic signals 11
3.2 NFAT transcription factor 12
3.3 Functional and therapeutical implications 13
HYPOTHESIS AND OBJECTIVES **14**
MATERIALS AND METHODS **14**
1. Primary hippocampal culture 14
2. Soluble Aβo preparation 15
3. Cell treatment, lysis and protein quantification 16
3.1 Cell treatment 16
3.2 Lysis and protein quantification 16
4. Immunoblotting 17
5. Immunocytochemistry 17
6. Confocal imaging and analysis 18
6.1 Cytosol to nucleus NFATc3 ratio 18
6.2 Dendritic PSD-95 spots and dendritic NFATc3 19
7. Statistical analysis 20
RESULTS **20**
1. Aβo effect on AKAP150 expression 20
2. Effect of LTCC blockade on Aβo-induced reduction of AKAP150 levels 21
3. Aβo effect on hippocampal secondary dendrites 22
3.1 Aβo effect on dendritic PSD-95 22
3.2 Aβo effect on dendritic NFATc3 23
4. Aβo effect on nuclear translocation of NFATc3 24
5. Aβo effect on phosphorylated NFATc3 26
DISCUSSION **26**
1. Alterations in AKAP150 induced by Aβo 27
2. Role of L-type calcium channels 27
3. Changes in PSD-95 and synaptic plasticity 28
4. Location and regulation of NFATc3 28
CONCLUSION **30**
REFERENCES **30**

INTRODUCTION

1. Alzheimer's disease

1.1 Alzheimer's overview

Alzheimer's disease (AD) is the most common form of dementia, taking up to 60-70% of cases (1). According to the World Health Organization, approximately 57 million people were affected by Alzheimer's in 2021, with nearly 10 million new cases arising every year (1).

Alzheimer's is an age-related disease that worsens over time. As the disease progresses, memory, communication and behaviour are affected, leading to confusion and loss of independence (2). In the final stages, it can also disrupt basic functions such as walking, talking or swallowing (2). Some of the main risk factors of the disease are age, hypertension, diabetes and being socially isolated (1). The latter is especially important among elderly people, given that loneliness and neglect of the aging population is one of the major issues in our society today.

The increase in life expectancy has contributed to a worldwide rise in AD cases, which represents an issue not only in health fields but also in the economic aspect (2). This situation entails an increment in resources directed towards medical treatments and patient care.

1.2 Neuropathology of the disease

AD brain degeneration starts before clinical symptoms appear, up to 20 years earlier (3). According to the actual disease model, the progression is divided in three main phases: a presymptomatic or preclinical phase, a prodromal phase (also called mild cognitive impairment (MCI)) and dementia due to AD (3). In the preclinical phase the patient still maintains a normal cognitive function even though pathological processes are underway. However, as time progresses, the damage defeats compensatory mechanisms and the first cognitive alterations appear. Finally, when this impairment affects everyday tasks, dementia can be diagnosed (3).

On a neuropathological level, the disease is characterized by two main lesions: the extracellular deposits of senile plaques formed by amyloid-beta peptide (Aβ) and the intracellular neurofibrillary tangles composed of hyperphosphorylated tau protein (4). Although both processes are considered key pathological markers, Aβ accumulation and aggregation is the one that initiates the process (Figure 1) (4).

Tau protein, the main component of NFT, plays a crucial role regulating microtubule stability and intracellular trafficking under basal conditions (4). However, in neuropathology, tau hyperphosphorylation is a key event. This process damages the microtubule-stabilizing function of tau, causing mislocalization in the somatodendritic region (3).

Aβ peptide is generated when an abnormal processing of amyloid-beta precursor protein (APP) occurs by β-secretase and γ-secretase enzymes. This process forms different isoforms of the peptide (3). Among them, Aβ1-42 is more prone to form toxic aggregates because of its low solubility (3). These sort of Aβ can create soluble

oligomers (Aβo) that are highly neurotoxic, which then become senile plaques (4). Several studies suggest that not all Aβo have the same level of toxicity. Depending on molecular weight, quaternary structure and relation to amyloid plaques two main subtypes of Aβo have been identified. Type 1 oligomers, also called high molecular weight (HMW) oligomers, exceed 50 kDa, are not directly related to senile plaques and are considered extremely toxic (5). On the contrary, type 2 oligomers or low molecular weight (LMW) oligomers, do not surpass 50 kDa and are temporally and structurally related to amyloid plaques (5). In comparison to HMW oligomers, the toxicity of LMW oligomers is significantly lower, and in some cases, have even been observed not to cause cognitive dysfunction (5).

Although the formation of neurofibrillary tangles by tau protein is also present in early stages of the disease, various articles have noted that Aβ accumulation accelerates the propagation of the tau pathology, augmenting the neuronal damage and the synaptic loss (3). Therefore, Aβ works as a trigger and an enhancer of the neurodegenerative process in AD (4).

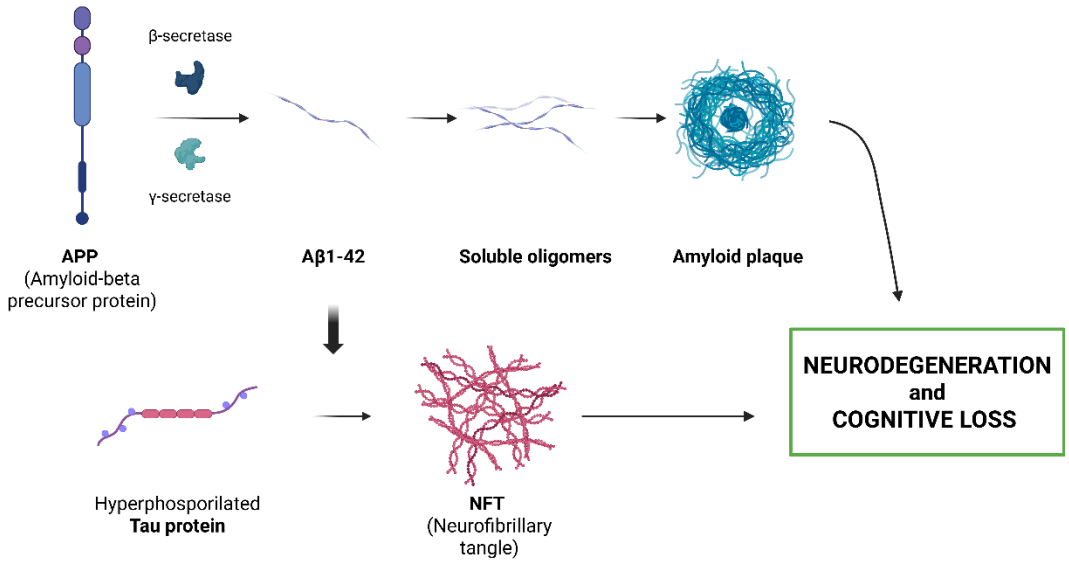

Figure 1. Neurodegeneration pathway, an overview of the two mayor lesions of AD: amyloid-β (Aβ) plaques and neurofibrillary tangles (NFT). Created with Biorender.

1.3 Diagnostic and treatment for Alzheimer's disease

Even though AD was historically diagnosed definitively through post-mortem neuropathological analysis of Aβ plaques and neurofibrillary tangles, current advances have introduced non-invasive tools and clinical methods of detecting the pathology on an early stage (6). Diagnostics are now mostly based on the combined use of biomarkers in cerebrospinal fluid (CSF) and in blood, and in neuroimages such as positron emission tomography (PET) (6).

The diagnostics criteria proposed by the National Institute on Aging and the Alzheimer's Association follows a classification based on biomarkers of beta-amyloid, Tau and neurodegeneration, called the AT(N) framework. This approach tracks AD from a preclinical stage to dementia, detecting biological changes even before clinical symptoms appear (6).

The most relevant biomarkers include Aβ42 or Aβ42/Aβ40 ratio and total Tau (t-tau) and hyperphosphorylated Tau protein in CSF (6). Furthermore, these biomarkers allow specific detection of p-tau181, p-tau217, neurofilament light chain (NfL) and glial fibrillary acidic protein (GFAP) in blood, which show a big correlation with the pathology and have a big predictive capacity for dementia development (7).

Regarding treatment, current pharmacological therapies mainly cover symptomatic aspects of the disease and focus on the cholinergic and glutamatergic systems. For mild to moderate AD cases acetylcholinesterase inhibitors like Donepezil (Arizept®), Rivastigmine (Prometax®) and Galantamine (Razadyne®) are approved (8). For moderate to severe stages of AD, N-methyl-D-aspartate receptor (NMDAR) non-competitive antagonist Memantine (Axura®) is accepted (8).

In recent years anti-amyloid immunotherapies have started to emerge. The Food and Drug Administration (FDA) approved monoclonal antibody Aducanumab® in 2021 (even though it was discontinued in 2024), followed by Lecanemab (Leqembi®) in 2023 and Donanemab (Kisunla®) in 2024 (9). These antibodies show different mechanisms of action: Lecanemab has stronger binding to soluble Aβ aggregates and Donanemab targets pyroglutamate-modified Aβ, binding to plaques (10).

Despite these advances, pharmacological treatment faces some major limitations, the main one being low brain bioavailability due to the blood-brain barrier (BBB) (8). New alternative strategies are being studied to counter this issue, such as the use of nanocarriers that can cross the barrier and act as drug delivery systems (8).

Nevertheless, it is important to consider that other potential therapeutic targets may exist that have not been studied enough. As of 2024, research included 187 clinical trials targeting different mechanisms of the pathology, including amyloid-beta, tau pathology and neuroinflammation (10). Further exploration could open new approaches for more effective and targeted interventions, which may become a key aspect for the development of truly disease-modifying treatments.

2. Synaptic plasticity alterations in Alzheimer's disease

2.1 Synaptic plasticity and physiological significance

Synaptic plasticity is a fundamental trait of the central nervous system that allows activity-dependant functional adaptation of neuronal connections (11). The hippocampus is one of the most important brain regions in the context of learning and memory, and two main mechanisms of long-term synaptic plasticity have been identified: long-term potentiation (LTP) and long-term depression (LTD) (11).

These plasticity forms rely on the activation of glutamate receptors α-amino-3-hydroxy-5-methyl-4-isoxazolepropionic acid (AMPARs) and NMDARs and are heavily regulated by molecular processes that include calcium entry, protein phosphorylation and dephosphorylation, cytoskeletal reorganization and gene expression modulation (12).

2.2 Molecular mechanisms of LTP and LTD

During LTP, a high-frequency stimulation induces a temporary but intense increase in intracellular calcium through NMDARs (13). This rise in calcium levels triggers an intracellular signalling cascade that results in the activation of some kinases, such as Ca2+/calmodulin kinase II (CaMKII), protein kinase A (PKA) and protein kinase C (PKC) (12). These enzymes phosphorylate different synaptic proteins, including AMPA receptor subunit 1 (GluA1) in specific residues (12). Ser845 is phosphorylated by PKA and Ser831 by both CaMKII and PKC (12). The phosphorylation of these residues increases the open probability of the channels and facilitates AMPARs trafficking to the synapses, increasing the glutamatergic synapse (12).

On the other hand, LTD is induced by a low-frequency stimulation that causes a reduced but constant increase of intracellular calcium that activates the calcineurin phosphatase (CaN) (13). CaN mediates the dephosphorylation of the Ser845 residue of GluA1, which targets these receptors for endocytosis from the synaptic membrane to intracellular compartments (12). This process produces a reduction in functional AMPARs at synapses, thus creating a decrease in synaptic efficiency. Additionally, CaN activation is also involved in actin cytoskeletal reorganization, which supports shrinkage of dendritic spines during LTD (14).

The balance between kinase phosphorylation and phosphatase dephosphorylation is key for synaptic plasticity, because it allows proper adaptation of the synapses (12). A misregulation in these mechanisms, driven by pathological agents such as oligomeric amyloid beta, could shift the balance towards a continuous synaptic depression, contributing to the functional decline observed in neurodegenerative diseases (15).

2.3 Oligomeric Aβ-induced synaptic dysfunction

In AD the balance between LTP and LTD is altered, resulting in synaptic disfunction (16). Evidence shows that soluble amyloid-beta oligomers (Aβo), especially Aβ1-42, directly interfere with synaptic plasticity by altering receptor function and key signalling proteins (17). For instance, it has been proved that Aβo disrupts NMDAR-dependant calcium influx, favouring LTD over LTP (16). Furthermore, Aβo can induce morphological changes in dendritic spines, leading to thinning or removal; this process is related to loss of synapse and cognitive decline (17).

One of the mechanisms by which Aβo induces a pathological LTD includes NMDAR subunit 2B (GluN2B) activation (17). This activation triggers a calcium influx that increases CaN activity, and this, in turn, supports the endocytosis of AMPAR which contributes to the decrease of synaptic efficacy (Figure 2) (16). This imbalance in synaptic signalling results in a maintained reduction of excitatory transmission.

Other than NMDARs and AMPARs, voltage-dependent calcium channels (VDCCs), especially L-type calcium channels (LTCCs), also participate in the entry of calcium and activation of intracellular signalling pathways (18). In the context of AD, these channels may be able to impact synaptic function and neuronal health due to alterations in calcium homeostasis, as an increased CaN activity is implicated in Aβ-

induced synaptic deficits (19). Because of that, these channels could represent an alternative strategy for the modulation of intracellular calcium in pathological conditions (19).

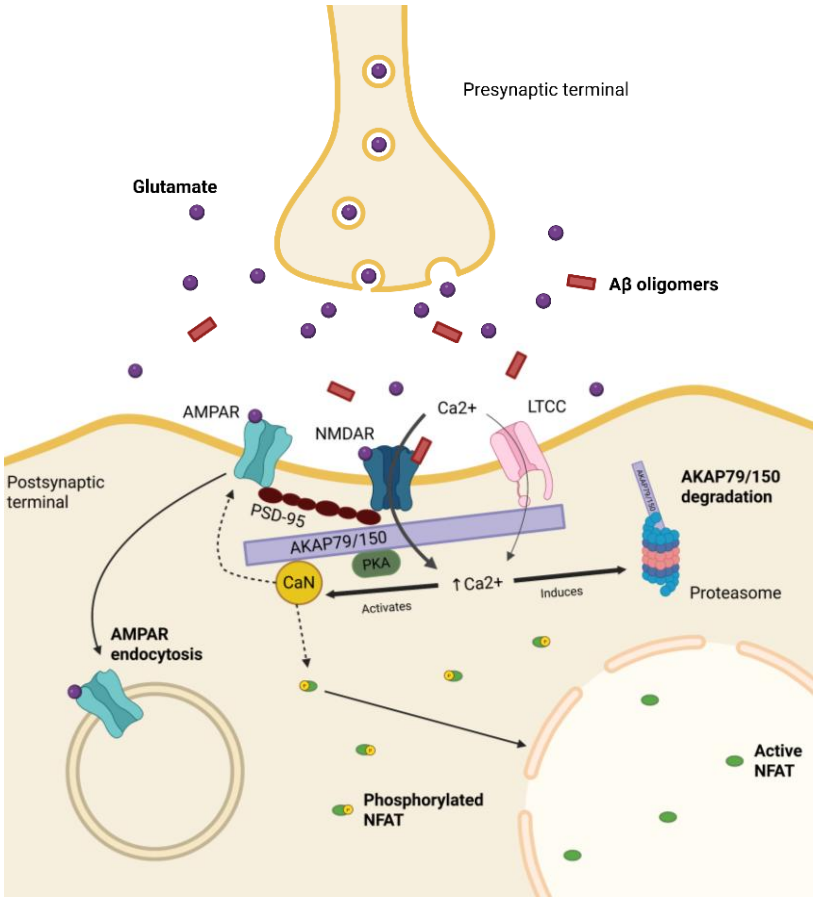

Figure 2. Aβo induced synaptic dysfunction in Alzheimer's disease. Aβ oligomers, especially Aβ1-42, alter synaptic homeostasis in the postsynaptic neuron. Aβo activates NMDAR (subunit GluN2B) and creates an aberrant increase in intracellular calcium. Along with calcium influx through LTCCs, this activates CaN, anchored by AKAP150, which dephosphorylates GluA1 and promotes endocytosis of AMPAR. Simultaneously, CaN activates transcription factor NFAT, which translocates to the nucleus and promotes degenerative-gene expression. Moreover, pathological intracellular calcium influx induces AKAP79/150 degradation by the ubiquitin-proteasome system. Created with Biorender.

3. Dysregulation of post-synaptic signalling complexes by Aβo

3.1 AKAP79/150 as an integrator of synaptic signals

A-kinase anchoring protein 79/150 (human/rodent) (AKAP79/150) is a scaffolding protein that organises multiproteic complexes in the postsynaptic region, anchoring kinases, such as PKA and PKC, and phosphatases like CaN (Figure 3) (20). AKAP70/150 regulates multiple aspects of synaptic signalling, including receptor phosphorylation, cytoskeletal reorganization and the dynamics of other anchoring proteins (20). This component is mainly localized in the dendritic spines, but it can also be found in other neuronal regions like proximal dendrites and soma (21).

AKAP79/150 is anchored in the plasma membrane by interactions with lipids, cortical actin and adhesion proteins, and it connects with AMPARs and NMDARs by

association with MAGUK scaffolds such as postsynaptic density protein 95 (PSD-95) (21). The whole complex works as a scaffold that organizes signalling pathways in specific parts of the cell. Furthermore, AKAP79/150 also possesses specific domains with direct interaction with LTCCs, allowing a more precise coordination and regulation of voltage-dependent calcium signals (20). Besides, PSD-95 is a MAGUK anchoring protein that regulates the organization of postsynaptic receptors, especially NMDARs as it binds to them with high affinity via its PDZ domains (22). In pathological conditions like AD, PSD-95 expression is reduced, and synaptic localization is altered, weakening spine architecture and glutamatergic transmission (22).

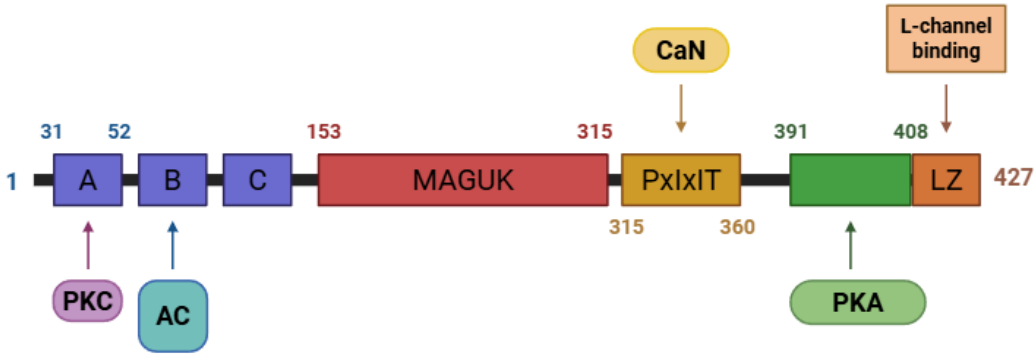

Figure 3. Structure of the AKAP79/150 anchoring protein. The N-terminal region binds to PKC and AC. Next, there is a domain that interacts with MAGUK family proteins, such as PSD-95. The PxIxIT motif allows binding to CaN, and another specific domain binds to PKA. In the C-terminal region, the leucine zipper (LZ) motif mediates the direct interaction with LTCCs. Created with Biorender.

In basal conditions, AKAP79/150 anchors PKA near GluA1, facilitating Ser845 phosphorylation and promoting AMPARs trafficking to the membrane (19). At the same time, AKAP also positions CaN phosphatase near the same substrates; this allows a bidirectional and dynamic regulation of synaptic plasticity depending on the intracellular activity (23). On the contrary, during LTD, AKAP79/150-bound CaN dephosphorylates GluA1, promoting AMPAR endocytosis (19).

Aβo-induced LTD causes a significant disruption by promoting AKAP79/150 degradation via the ubiquitin-proteasome system (Figure 2) (23). This interrupts the precise localization of both PKA and CaN, and disrupts the fine regulation of the GluA1 phosphorylation, resulting in the decrease of membrane AMPARs and the loss of phosphorylated GluA1 (24).

3.2 NFAT transcription factor

Transcription factors are dynamic regulatory proteins that have high levels of cellular mobility depending on physiological stimuli. An example of this mechanisms is the CREB family, with proteins distributed throughout the cell in basal conditions but capable of nuclear translocation to control transcriptional activity (25). Other transcription factors like Nr4a2 also show dynamic cellular movement, being found not only in nuclear and cytoplasmic regions, but also in synaptic locations (26).

Transcription factors are not static molecules, as shown by these examples, but dynamic cellular components that integrate different signals and inputs to coordinate appropriate gene-expression.

Nuclear factor of activated T-cells (NFAT) is a family of transcription factors composed of 5 members: NFAT1 (also known as NFATc2), NFAT2 (NFATc1), NFAT3 (NFATc4), NFAT4 (NFATc3) and NFAT5 (TonEBP) (27). Most of these factors, except for NFAT5 that activates through osmotic stress, are activated by a CaN-dependent dephosphorylation in Ser165 (27). Under basal conditions, they remain phosphorylated and inactive in the cytoplasm. However, when a maintained increase in intracellular calcium happens (mediated by calcium entrance through LTCCs and NMDARs) NFAT is dephosphorylated by CaN and translocates to the nucleus (Figure 2) (18). There, it regulates the expression of genes related to synaptic degeneration, like Mdm2, which supports spine loss in dendrites (24). NFAT factors are expressed in various tissues, including the brain, with NFATc3 specifically located in hippocampal neurons (28).

3.3 Functional and therapeutical implications

Aβo-induced alterations in the AKAP79/150-CaN-NFAT signalling pathway have consequences throughout different regions of the synapse, from receptor trafficking to gene transcription (24). These elements may be considered as possible therapeutical targets (29). Under basal conditions, this complex organizes and regulates LTCC-dependent calcium entry, which, through a dynamic balance between PKA and CaN activity, modulates NFATc3 phosphorylation and controls its gene expression (20).

In exposition with Aβo, AKAP79/150 is degraded by the ubiquitin-proteasome system, which alters this synaptic organization (23). The loss of AKAP79/150 impairs the binding of CaN and PKA to LTCCs, generating a dysregulation of their activity (20). In absence of this regulation, these channels may hyperactivate, facilitating an aberrant increase in calcium influx that excessively activate CaN. This, in turn, induces a pathological dephosphorylation of NFATc3, favouring nuclear translocation and transcription of degenerative genes contributing to the progressive synaptic loss (24).

Furthermore, modulating LTCC activity or interfering in AKAP-CaN-NFAT complex could restore signalling equilibrium and limit the expression of neurodegenerative genes. That is why LTCCs could provide a pharmacological means to control the balance between calcium-mediated phosphorylation and dephosphorylation (24).

These pathways could be pharmacologically interfered, expanding the range of AD investigation (24). Moreover, a detailed study could achieve the development of specific biomarkers that indicate the functional state of the synapse, allowing more precise and earlier diagnostic of AD or even new therapeutical strategies for the disease (29). In summary, AKAP79/150, NFAT and LTCCs rise as three key factors whose dysregulation contributes to synaptic decline, and whose manipulation could diminish, at least partially, the course of the disease (29).

HYPOTHESIS AND OBJECTIVES

According to previous studies, Aβo cause functional alterations in different neuronal signalling pathways related to AD. The hypothesis of this study postulates that Aβ oligomers induce a disruption of the AKAP79/150-CaN-NFAT signalling pathway, altering expression and function of AKAP79/150 scaffolding protein and inducing altered distribution in NFATc3.

To assess this hypothesis, the main planned objectives are:

1. To study the alterations in the expression of AKAP79/150 by Aβo.

2. To determine the role of voltage-dependent calcium channels in Aβo-induced AKAP150 degradation.

3. To investigate the effects of Aβo on the cellular localization and dendritic distribution of NFATc3.

MATERIALS AND METHODS

1. Primary hippocampal culture

Hippocampal neurons were obtained from C57BL/6JRccHsd mice pups at postnatal day 0-2 (P0-P2).

Firstly, 12- and 24-well plates (Falcon®) were prepared. For immunocytochemistry, 12mm diameter coverslips (Deckgläser No.1) were placed in the wells of 24-well plates. They were previously treated with 8% chlorohydric acid in distilled water and kept overnight with gentle agitation. The coverslips were washed, kept in ethanol and sterilized by using a Bunsen burner and 15-minute UV irradiation.

At least 2 hours before plating the cells, the wells were pre-coated with 500µL of poly-D-lysine (PDL) (Table 1) mixture to ensure the adhesion of the neurons. Then, the wells were washed with PBS 1X (Table 1) and finally replaced by supplemented Neurobasal-A medium (Table 1).

To prepare the dissociated hippocampal cultures, the mice pups were decapitated at postnatal day 0-2 and placed into cold dissection solution (Table 1). Hippocampi were isolated and incubated into an enzymatic solution (Table 1) that was previously sterilized by using 0,2µm filters (FiltroPur 0.2) for 30 minutes. Before the trituration of the hippocampi, inactivation solution (Table 1) was added for 2 minutes. Then, the tissue was mechanically dissociated in serum media (Table 1) by using a fire-polished glass Pasteur pipette and a nylon mesh (40 µm pore size). When trituration was complete, cells were centrifuged for 5 minutes at 1000 rpm. The pellet was then resuspended in serum media; neurons were counted in a Neubauer hemocytometer and then plated in the wells with pre-warmed cultured medium.

The cells were plated in specific densities depending on the experiment. For Western blot analysis, cells were plated in 12-well plates at 250.000 cells per well, and for immunocytochemistry experiments, the optimal density was 125.000 cells per well in 24-well plates containing coverslips.

The neuronal cultures were incubated in a humified incubator at 37ºC with 5% CO2 and 95% air. Half of the culture medium was replaced the following day after plating, and every 7 days after the procedure (Figure 4). To prevent glia-overgrowth, the mitotic inhibitor 5-fluorodeoxyuridine (FDUR) (Table 1) was added to the wells at 2-3 days in vitro (DIV2-3); for both 24-well plates and 12-well plates 5 µl were added.

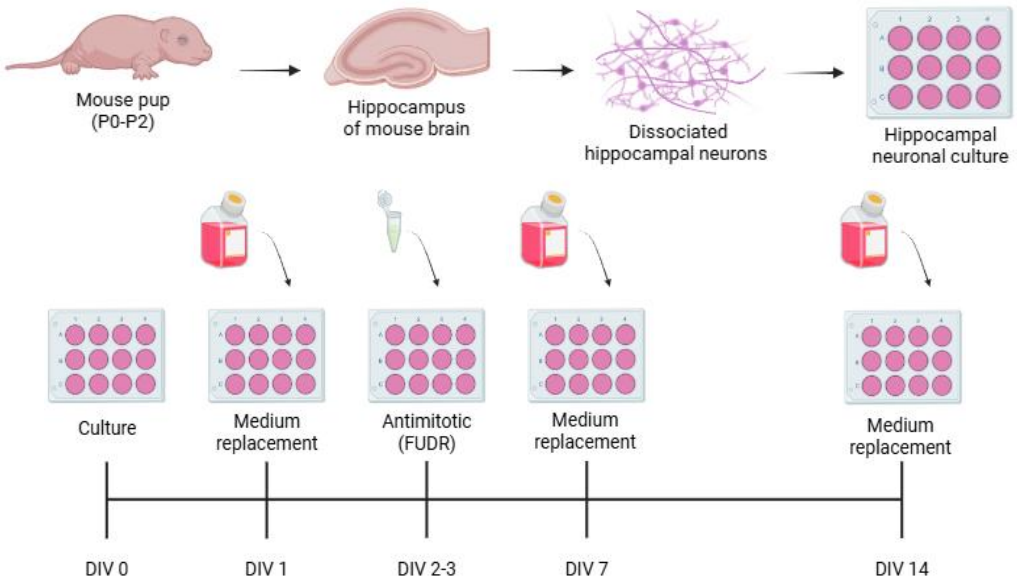

Figure 4. Experimental timeline of the neuronal culture. Created with Biorender.

Table 1. Composition of media and solutions used for primary hippocampal cultures.

SOLUTION	COMPOSITION
PDL buffer	Poli-D-lysin diluted in 0,1M Sodium Borate buffer pH 8.4
Supplemented Neurobasal-A medium	Neurobasal-A medium (Thermo Fisher Scientific) supplemented with 10 mL B27 and 5 mL GlutaMAX (Thermo Fisher Scientific)
Dissection Solution	160g NaCl, 4.96g KCl, 1g MgSO4, 3.87g CaCl2, 5g HEPES, 5.55g glucose, 5.64 x 10-3 mM phenol red
Serum Media	Minimum Essential Medium (MEM) with Earle's salts without L-glutamine (Thermo Fisher Scientific) supplemented with 5% (FBS), 21 mM glucose and 1 mL mito + serum extender (Corning)
Enzymatic Solution (10 mL)	10 mL of dissection solution supplemented with 2 mg L-cysteine, 100 µL ethylenediaminetetraacetic acid (EDTA) (50 mM, pH 8), 100 µL CaCl2 (100mM), 15 µL NaOH (1N), 100 µL papain (100 units) (Worthington) and 100 µL DNase I (300 – 450 Kunitz / mL) (Sigma)
Inactivation Solution (10 mL)	10 mL of serum media supplemented with 25 mg BSA and 100 µL DNase I
FUDR	100 mg 5-Fluoro-2'Deoxyuridine (Sigma) and 250 mg uridine (Sigma) in 50 ml MEM with Earle's salts without L-glutamine
PBS 10x	80g NaCl, 2g KCl, 11.5 g Na2HPO4 · 7H2O (S-9390 Sigma), 2gr KH2PO4 (P-5379 Sigma); pH 6.9
PBS 1x	Dilution 1/10 PBS 10x; pH 7.4

2. Soluble Aβo preparation

The preparation of soluble amyloid-beta oligomers was made following the protocol described by Fa et al. (2010) (30).

To obtain a 5 mM stock solution of amyloid-beta oligomers, synthetic Aβ1-42 peptide (GenicBio) was dissolved in dimethyl sulfoxide (DMSO). The solution was sonicated in a water bath sonicator for 10 minutes and was aliquoted into low-binding protein tubes (Eppendorf®). Finally, the aliquots were stored at -20ºC.

The stock was then diluted to 100 µM using cold DMEM/F-12 medium without phenol red (Gibco®). Afterwards, the solution was vortexed for 30 seconds and incubated at 4ºC for 12 hours, to ensure the formation of the oligomers. After incubation, a final concentration of 5 µM of oligomers diluted in artificial cerebrospinal fluid (ACSF) was used for cell treatment.

3. Cell treatment, lysis and protein quantification

On DIV16, neuronal cultures were treated and lysed.

3.1 Cell treatment

Before treatment, the culture medium was removed, and neurons were pre-incubated for 30 minutes with ACSF (Table 2) containing calcium and magnesium to mimic biological conditions. Basal and Aβo groups received ACSF alone, while the nimodipine (NIMO) groups received ACSF with 10 µM nimodipine.

After the pre-incubation, neurons were treated for 10 minutes with ACSF lacking magnesium (ACSF -Mg) (Table 2). The basal group received ACSF -Mg alone, the Aβo group received ACSF -Mg with 5 µM Aβo, and the nimodipine groups received ACSF -Mg with their respective treatments (Aβo + nimodipine or nimodipine alone).

Following treatment, neurons were incubated again in ACSF with calcium and magnesium for 50 minutes, with nimodipine groups receiving ACSF with nimodipine.

In addition to that, another group of neurons were exposed to Aβo for 3 hours. Pre-treatment consisted in 30 minutes with ACSF, followed by a treatment of 10 minutes with ACSF -Mg containing 5 µM Aβo. Finally, the neurons were again incubated with ACFS for additional 2 hours and 50 minutes prior to lysis.

3.2 Lysis and protein quantification

After treatment, cultures were lysed in cold RIPA-lysis buffer (Table 2) and drawn with a scrapper.

To determine the protein concentration of samples, the Pierce BCA protein assay kit (Thermo Fisher Scientific) was used. A calibration curve was obtained by using Albumin (Thermo Fisher Scientific) at serial concentrations (1 mg/ml, 0,667 mg/ml, 0,5 mg/ml, 0,33 mg/ml, 0,25 mg/ml, 0,167 mg/ml, 0,125 mg/ml, 0,083 mg/ml, 0,0625 mg/ml, 0,042 mg/ml) and samples were diluted 1/10. Reagent B was diluted 1:50 in reagent A and standards and samples were incubated at 37ºC for 30 minutes. After that, the samples were analysed at 562 nm by using a spectrometer.

The amount of protein calculated with BCA was diluted in H2O and sample loading buffer 4X (LI-COR 928-40004 + 10% β-mercaptoethanol). Samples were kept at -20ºC.

4. Immunoblotting

After preparing the samples with BCA process, they were heated at 96ºC for 4 minutes. Samples were loaded to pre-made gels (Odyssey Mini Precast Gels, LICORbio) and separated by electrophoresis in running buffer 1X (Odyssey MOPS SDS Running Buffer Powder reconstituted in 1000ml of distilled water, LICORbio). Next, proteins were transferred to nitrocellulose membranes (Cytiva) in transfer buffer 1X (Odyssey Transfer Buffer Powder reconstituted in 800ml of distilled water and 200ml of ethanol, LICORbio). Membranes were then stained with 0,1% Ponceau S solution (Sigma) to verify correct transference. Afterwards, membranes were blocked 1 hour in blocking buffer (Table 2), washed in PBS-Tween 20 (PBS-T) (Table 2) twice for 5 minutes and twice for 10 minutes and incubated at 4ºC overnight with primary antibodies (Table 3) mixed with antibody solution (Table 2). The next day, membranes were washed in PBS-T, incubated for 1 hour at room temperature with 1/1000 secondary antibodies diluted in blocking buffer (anti-mouse, anti-rabbit horseradish peroxidaseconjugated (HRP) IgG for Chemiluminescence detection and anti-mouse, anti-rabbit IRDye 680 and 800 for Fluorescence detection) and washed in PBS-T.

Membranes were analysed using Chemiluminescence, with ECLTM Western blotting Detection Reagents (GE Healthcare) and Odyssey Fc Imaging System (LICORbio) and using Fluorescence, with the Odyssey M Imaging System. The densitometry of the membranes was performed using Fiji-ImageJ v2.0 (National Institutes of Health, Bethesda, MD), and protein levels were corrected with GAPDH as loading control.

Table 2. Composition of solutions used for cell treatment, lysis and immunoblotting.

SOLUTION	COMPOSITION
ACSF Ca2+/Mg2+	125 mM NaCl, 2.5 mM KCl, 1 mM MgCl2, 2 mM CaCl2, 33 mM D-Glucose, 25 mM HEPES (pH 7.3; 320mosM final)
ACSF Ca2+/-Mg2+	125 mM NaCl, 2.5 mM KCl, 2 mMCaCl2, 33 mM D-Glucose, 25 mM HEPES (pH 7.3; 320mosM final)
RIPA lysis buffer	50 mM Tris Base pH 7.4, 150 mM NaCl, 2mM EDTA, 1 % NP-40, 0,5 % Triton X-100, 0,1 % SDS, 1 mM Na3VO4, 25mM NaF, 1mM PMSF, protease (1/100) and phosphatase inhibitors (1/100)
Blocking solution pH 7,4	10% dried milk, 0,1% BSA in PBS 1X; pH 7,4
PBS-T	0,05% Tween-20 in PBS 1X
Antibody dilution buffer	0,1% BSA, 0,02 thimerosal in PBS 1X

5. Immunocytochemistry

Hippocampal neurons plated on 24-well plates containing glass coverslips were washed at 16 DIV with 500 µl PBS 1X (Table 1) and fixed with 400 µl of PFA solution (4% PFA and 4% sucrose in PBS 1X) for 15 minutes at 4ºC. After fixation, cells were washed with cold PBS 1X and stored at 4ºC in PBS 1X until immunodetection.

Neurons were permeabilized with 0,1% Triton X-100 in PBS 1X (500 µl per well) for 20 minutes at room temperature and blocked in 500 µl of 2% normal goat serum (Sigma) in PBS 1X for 20 minutes at 37ºC with gentle agitation. After blocking, neurons were incubated for 1 hour at 37ºC in soft agitation with primary antibodies

(Table 3) diluted in 150 µl blocking buffer. After washing with PBS 1X, cells were incubated with specific Alexa Fluor secondary antibodies (1/500 goat anti-mouse Alexa-488 and 568, Thermo Fisher Scientific) diluted in blocking buffer for 1 hour at 37ºC in gentle agitation and protected from light.

Afterwards, cells were washed with PBS 1X and incubated for 5 minutes with the nuclear marker Hoechst 33258 (1:10,000; Thermo Fisher Scientific) diluted in 500 µl PBS 1X. Finally, neurons were washed again with PBS 1X and mounted in Fluoromont G mounting medium (SouthernBiotech).

6. Confocal imaging and analysis

Images were acquired using a Zeiss LSM700 Laser-Scanning microscope (Carl Zeiss Microscopy, Jena, Germany). They were taken using 63X immersion oil objectives, at 16 bits and 1024 x 1024 resolution for cytosol-to-nucleus NFATc3 ratio analysis and 1024 x 350 resolution for dendritic analysis. Settings for photomultiplier voltage, gain master and offset were optically adjusted to obtain minimum saturation and sequential frame acquisition was set to acquire 10 slices of 0.4 µm/slice.

Images were analysed using ImageJ 2.0v or Imaris 8 software.

6.1 Cytosol to nucleus NFATc3 ratio

For NFATc3 localization analysis, the images used contained two fluorescent channels (DAPI and NFATc3) and were processed using ImageJ software. The DAPI tinction was used to delimit the nuclear regions of interest (ROIs), that were manually selected and saved. The NFATc3 channel was duplicated to obtain two versions: one of them to represent the nucleus and the other one the cytoplasm. The cytoplasmatic signal was removed in the nuclear image by using the “Clear outside” tool, while the nuclear signal in the cytoplasmatic image was eliminated with “Clear” tool. (Figure 5) Finally, mean intensity values were measured, and the cytosol/nucleus ratio was calculated by dividing cytosolic intensity and nuclear intensity.

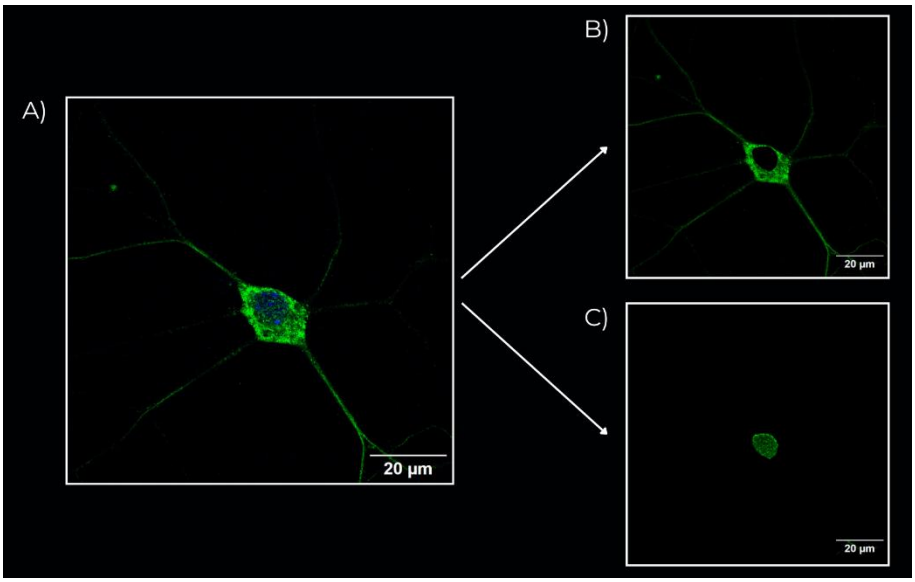

Figure 5. Segmentation and intensity analysis of cytoplasmic and nuclear NFATc3 in neurons. A) Hippocampal neuron at 16 DIV. NFATc3 is shown in green and nucleus in blue. B) Segmentation of cytoplasmic NFATc3. C) Segmentation of nuclear NFATc3. Scale bar: 20µm.

6.2 Dendritic PSD-95 spots and dendritic NFATc3

For the quantification of dendritic signals of PSD-95 and NFATc3, secondary dendrites were selected due to their more homogeneous morphology comparing to primary dendrites. Confocal images were processed with the Imaris 8 software (Bitplane, Oxford instruments), as it provided detailed spatial information of the samples and allowed a three-dimensional analysis.

PSD-95 spot detection was achieved maintaining a constant threshold and quality. A surface grain size of 0,0662 µm was applied, and a spot diameter of 0,5 µm was set, enabling the option of “Split touching objects” to differentiate the spots. The minimal number of voxels per spot was 10. Once the analysis was performed, the total amount of PSD-95 spots was obtained for each dendrite (Figure 6C and F).

For the study of dendritic NFATc3 a manual threshold was selected, and smoothing was enabled with a value of 0,1 µm. A minimum of 10 voxels was stablished, and the option of “Split touching objects” was disabled. In this case, all values (not averages) were extracted, area, volume and intensity of every selected dendrite (Figure 6D and G).

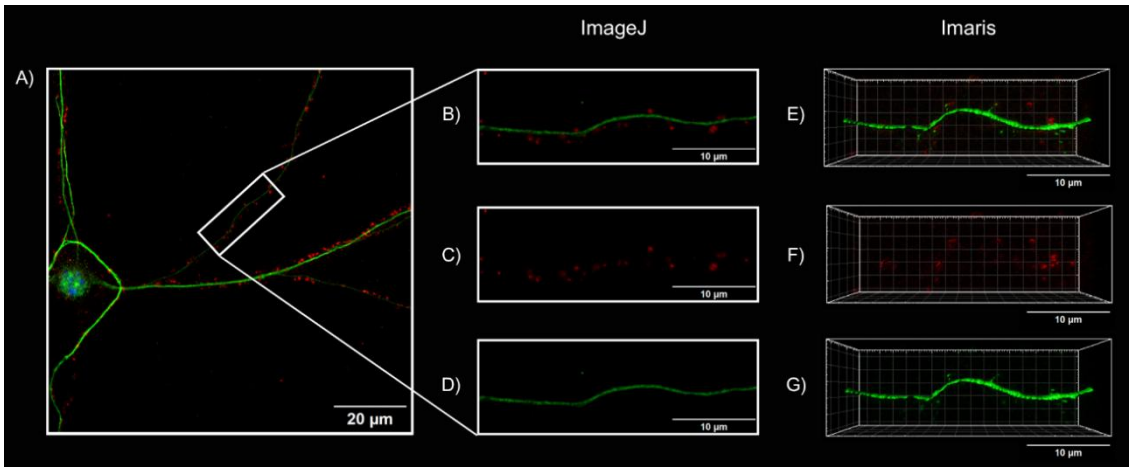

Figure 6. Processing of dendritic selection and channel separation. A) Hippocampal neuron at 16 DIV. NFATc3 is shown in green, PSD-95 in red and nucleus in blue. B) Secondary dendrite shown in ImageJ, PSD-95 in red and NFATc3 in green. C) Dendritic PSD-95 spots in ImageJ. D) Dendritic NFATc3 signal in ImageJ. E) Secondary dendrite shown in Imaris. F) Dendritic PSD-95 spots in Imaris. G) Dendritic NFATc3 signal in Imaris. Scale bar (A): 20µm. Scale bar (B-D): 10µm.

Table 3. List of primary antibodies used for Western Blot and immunocytochemistry.

ANTIBODY	SOURCE	DILUTION	TECHNIQUE
Mouse monoclonal anti-GAPDH	Invitrogen (AM4300)	1/10000 in antibody dilution	Western Blot
Rabbit polyclonal anti-AKAP150	Santa Cruz Biotechnology (sc-10765)	1/1000 in antibody dilution	Western Blot
Rabbit polyclonal anti-pNFATc3	Invitrogen (PA5-104980)	1/500 in antibody dilution	Western Blot
Mouse monoclonal anti-PSD95	Abcam (ab2723)	1/500 in antibody dilution	Immunocytochemistry
Rabbit polyclonal anti-NFATc3	Invitrogen (PA5-99546)	1/250 in antibody dilution	Immunocytochemistry

7. Statistical analysis

Statistical analysis was performed using GraphPad Prism software v8.0.1 (GraphPad Software Inc., California, USA). Firstly, normality of data was assessed by a Shapiro-Wilk test. When data met requirements for parametric tests, analyses of variance (one-way ANOVA) followed by Tukey's multiple comparisons test were performed. When normality or variance requirements failed, Kruskal-Wallis test followed by Dunn's multiple comparisons test was used. Data is represented as the mean ± standard deviation (SD). Statistically significant difference was set at p-value < 0.05 and is indicated as follows: *p< 0.05, **p< 0.01, ***p< 0.001, ****p< 0.0001.

RESULTS

1. Aβo effect on AKAP150 expression

Previous studies state that there is a decrease in AKAP150 expression after exposure to amyloid-beta oligomers (23). We decided to test whether this effect also

happened in a time-dependent manner up to three hours. A Western-blot analysis was performed on cultured hippocampal neurons. Cells were treated with oligomers for either 1 hour or 3 hours (see materials and methods section 3.1) and neurons maintained in basal conditions (untreated) were used as control. Representative blots of AKAP150 (upper blot) and GAPDH (lower blot) show protein levels across treatments (Figure 7A).

Quantification of AKAP150 protein levels showed that Aβo significantly reduced the expression of AKAP150 after 3 hours of treatment compared to basal conditions (p=0,0291), which correlates with the previously obtained results that demonstrated a decrease in its expression. A non-significant reduction was observed at 1 hour (Figure 7B). These results suggest a time-dependent effect of Aβo on AKAP150 protein levels.

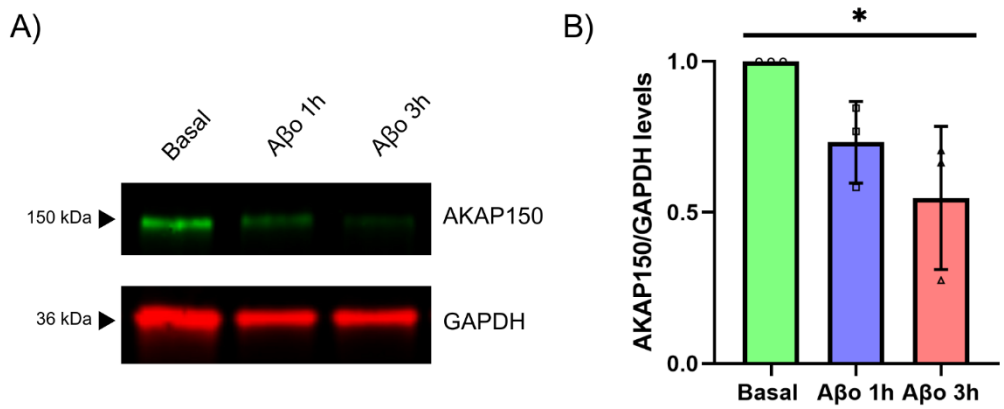

Figure 7. Aβ oligomers reduce AKAP150 expression in 16 DIV hippocampal neurons. A) Representative blots showing AKAP150 levels (upper blot) and GAPDH protein levels (lower blot) in neurons under basal conditions or treated with Aβo for 1 hour or 3 hours. B) Quantification of the AKAP150/GAPDH ratio. Data represent mean ± SD (n=3). *p<0.05. Statistical analysis was determined by one-way ANOVA followed by Tukey's post hoc test.

2. Effect of LTCC blockade on Aβo-induced reduction of AKAP150 levels

Once we proved that AKAP150 was reduced in presence of Aβo, we decided to test if this decrease depended on L-type calcium channels, given that AKAP150 regulates their activity and is directly bound to them (18). To study the involvement of LTCCs a Western blot analysis was performed on cultured hippocampal neurons following treatment with 4 different conditions: basal (untreated), Aβo treatment for an hour, combined treatment of Aβo and LTCC blocker nimodipine, and nimodipine treatment alone (see materials and methods section 3.1). Representative blots of AKAP150 (upper blot) and GAPDH (lower blot) show protein levels across treatments (Figure 8A).

Quantification of AKAP150 protein levels revealed no statistically significant differences between conditions. However, a decrease in AKAP150 levels was observed in Aβo-treated group compared to basal, and this decrease was similar to the one happening with Aβo + nimodipine group. Moreover, nimodipine treatment

alone showed an increase of AKAP150 levels compared to Aβo-group, although these levels did not reach basal group values (Figure 8B).

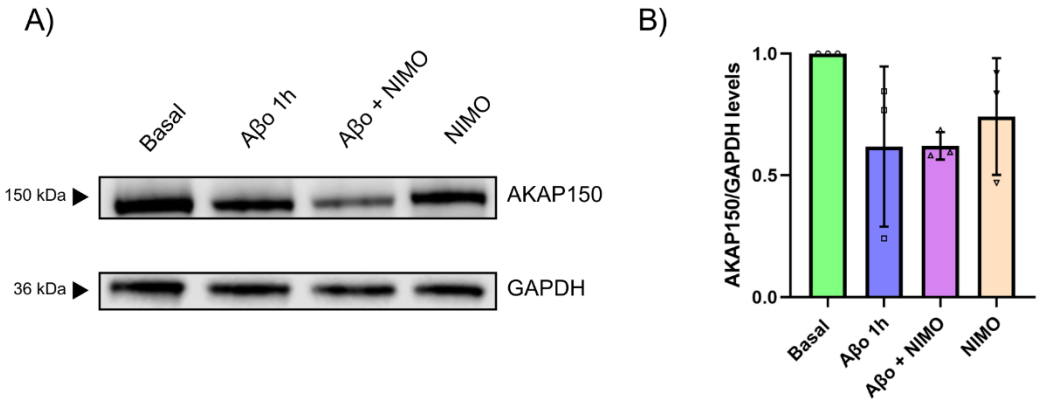

Figure 8. Modulation of AKAP150 levels in hippocampal neurons after exposition with Aβo and calcium channel blockade. A) Representative blots showing AKAP150 levels (upper blot) and GAPDH protein levels (lower blot) in neurons under basal conditions or treated with Aβo for 1 hour, Aβo + nimodipine, or nimodipine. B) Quantification of the AKAP150/GAPDH ratio. Data represent mean ± SD (n=3). Statistical analysis was determined by one-way ANOVA followed by Tukey's post hoc test.

3. Aβo effect on hippocampal secondary dendrites

To investigate the effect of Aβ oligomers on dendritic NFATc3 distribution and PSD-95 spots in hippocampal neurons, a three-dimensional analysis was performed using Imaris software. The procedure for treatment of the neurons, immunocytochemistry, imaging and analysis is specified in materials and methods.

3.1 Aβo effect on dendritic PSD-95

As a preliminary step before analysing AKAP-CaN-NFAT complex in dendrites, we decided to evaluate the synaptic condition of the neurons in presence of Aβo. PSD-95 was used as a synaptic marker quantifying spots in dendrites through a three-dimensional model. In representative images, PSD-95 spots are shown across the three conditions, basal, Aβo 1 hour and Aβo 3 hours (Figure 9A).

Quantitative analysis revealed a significant decrease in the number of PSD-95 spots in the Aβo-treated 1-hour group, both in comparison to basal group (p=0,0042) and 3-hour group (p<0,0001). No statistical differences were spotted between basal and 3-hour groups, even though a remarkable variability was found in these two conditions between samples. Furthermore, although the difference does not reach statistical significance, a tendency towards more PSD-95 spots appeared in the 3-hour group comparing to basal, a pattern not commonly described in literature (Figure 9B).

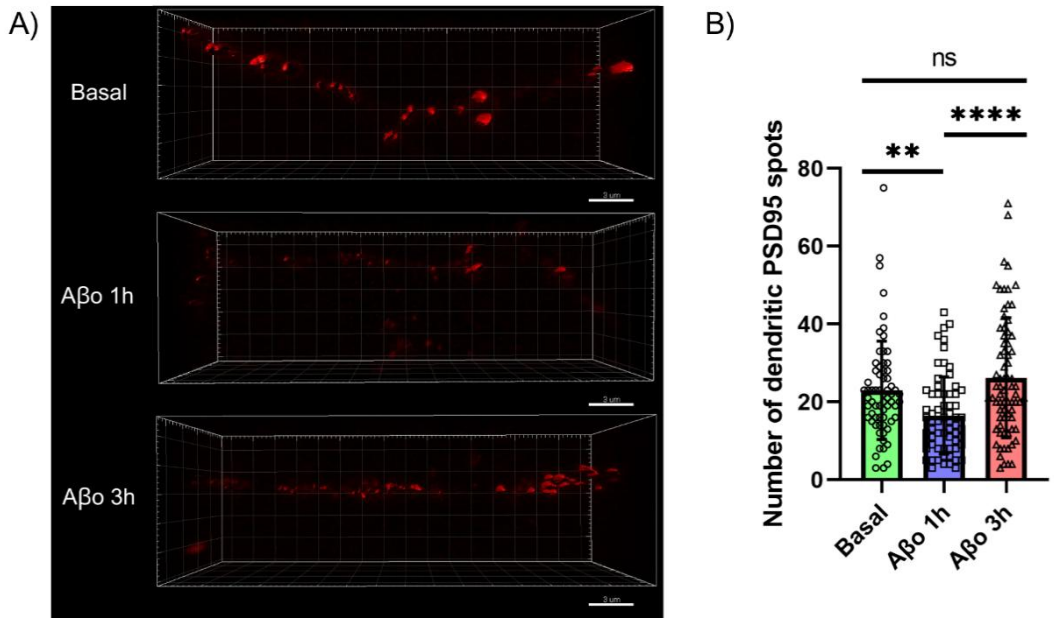

Figure 9. Aβ oligomers create a transient reduction of PSD95 spots in secondary hippocampal dendrites. A) Representative 3D reconstruction of PSD-95-stained dendrites, under basal conditions or treated with Aβo for 1 hour or 3 hours using Imaris software. Scale bar: 3µm. B) Quantification of dendritic PSD-95 spots. Data represent mean ± SD (n≈68 dendrites/group from 2 independent cultures). **p<0.01, ****p<0.0001. Statistical analysis was determined by Kruskal-Wallis test followed by Dunn's multiple comparisons test.

3.2 Aβo effect on dendritic NFATc3

Recent publications have reported that, after Aβo exposition, NFATc3 translocates to the nucleus to induce neurodegenerative gene expression (24). To understand how Aβo affects AKAP-CaN-NFAT in postsynaptic regions, we analysed dendritic distribution of the transcription factor. Representative 3D images show NFATc3 signal across dendrites from the three different groups (basal, Aβo 1h and Aβo 3h) (Figure 10A). Quantitative analysis of NFATc3 signal was represented in three different parameters: occupied area, volume and mean fluorescence intensity.

Firstly, the occupied area of NFATc3 showed a significant decrease in the 1-hour Aβo-treated group compared to both basal group (p=0,0002) and 3-hour group (p=0,0019). No significant differences were spotted between basal and 3-hour groups (Figure 10B).

In a similar way, the dendritic NFATc3 volume was also significantly reduced after 1 hour of treatment when compared to both the basal (p<0,0001) and 3-hour group (p=0,0017), with no significant differences between basal and 3-hour conditions (Figure 10C).

Finally, mean NFATc3 fluorescent intensity followed the same pattern: a significant decrease at 1-hour treatment with Aβo compared to basal (p<0,0001) and 3-hour (p=0,0069) groups. No statistical differences were spotted between control and Aβo 3 hours (Figure 10D).

It is worth mentioning that although the basal group generally showed higher average NFATc3 signal throughout the analyses, elevated variability was observed in this condition compared to the Aβo-treated groups.

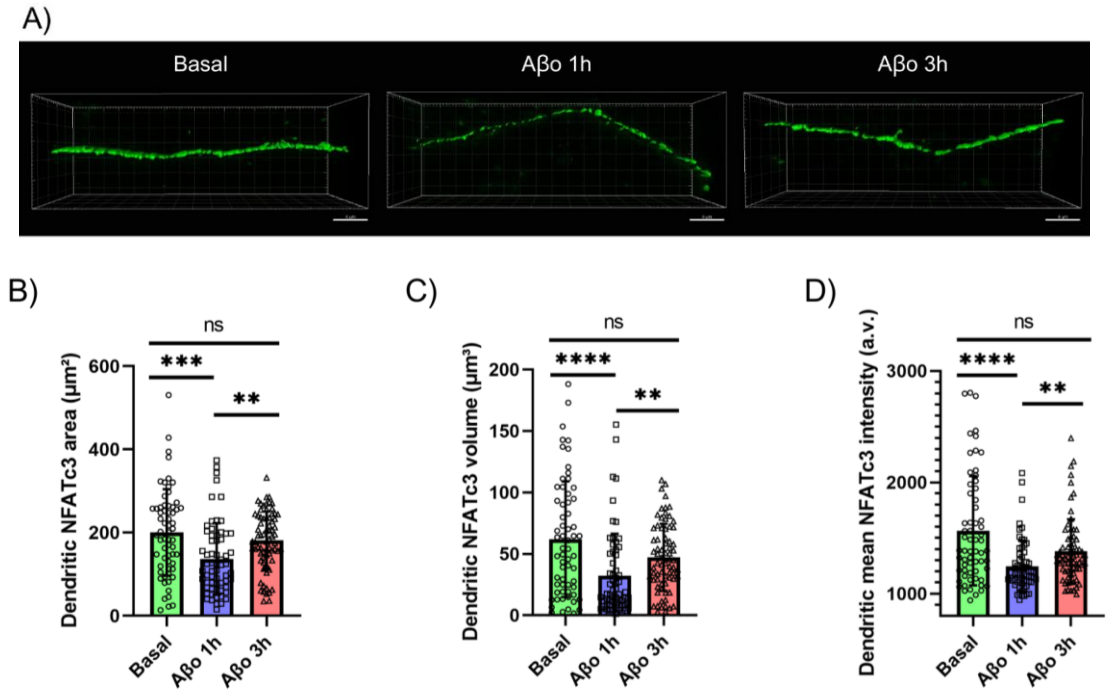

Figure 10. Aβ oligomers modulate dendritic distribution of NFATc3 in secondary hippocampal dendrites. A) Representative 3D reconstruction of NFATc3-stained dendrites, under basal conditions or treated with Aβo for 1 hour or 3 hours using Imaris software. Scale bar: 4µm. (B-D) Quantification of dendritic NFATc3: B) area C) volume and D) mean fluorescent intensity. Data represent mean ± SD (n≈66 dendrites/group from 2 independent cultures). **p<0.01, ***p<0.001, ****p<0.0001. Statistical analysis was determined by Kruskal-Wallis test followed by Dunn's multiple comparisons test.

4. Aβo effect on nuclear translocation of NFATc3

After dendritic analysis, we wanted to determine whether the NFATc3 that left the dendrites translocated to the nucleus, as literature supports (24). To assess the cellular location of the transcription factor, we analysed both cytoplasm and nuclei of the neurons. Cells were treated with Aβo for either 1 hour or 3 hours, maintaining a basal group untreated as control (see materials and methods section 3.1). The neurons were then fixed (see materials and methods section 5) and incubated with anti-NFATc3 antibody as well as Hoechst to mark the nucleus.

Under basal conditions and after 1 hour of Aβo treatment NFATc3 signal was similarly distributed (Figure 11A). In contrast, the 3-hour group displayed a big heterogeneity in the localization of NFATc3 signal. To represent this, two images are shown, one in which a diffuse NFATc3 distribution can be seen throughout the neuron (upper image), and another where the NFATc3 signal is clearly accumulated in the nucleus (lower image).

Quantitative analysis of cytoplasmic mean NFATc3 fluorescence intensity revealed a decrease in intensity in the 1-hour group treated with Aβo (p=0,348) compared to basal and a major decrease compared to the 3-hour group (p<0,0001) (Figure 11B).

Regarding nuclear mean NFATc3 fluorescent intensity, significant reduction was observed in both 1-hour (p=0,0014) and 3-hour (p=0,0399) treatment comparing to basal (Figure 11C). The analysis of cytosolic-to-nuclear fluorescent intensity ratio of NFATc3 showed a significative increase in neurons treated with Aβo for 3 hours compared to both basal group (p=0,0002) and the 1-hour group (p=0,0098) (Figure 11D).

Nevertheless, the 3-hour group also showed an elevated variation between neurons in all the analyses, the values raging from the highest to the lowest of all samples, reflecting the heterogeneity observed in confocal images.

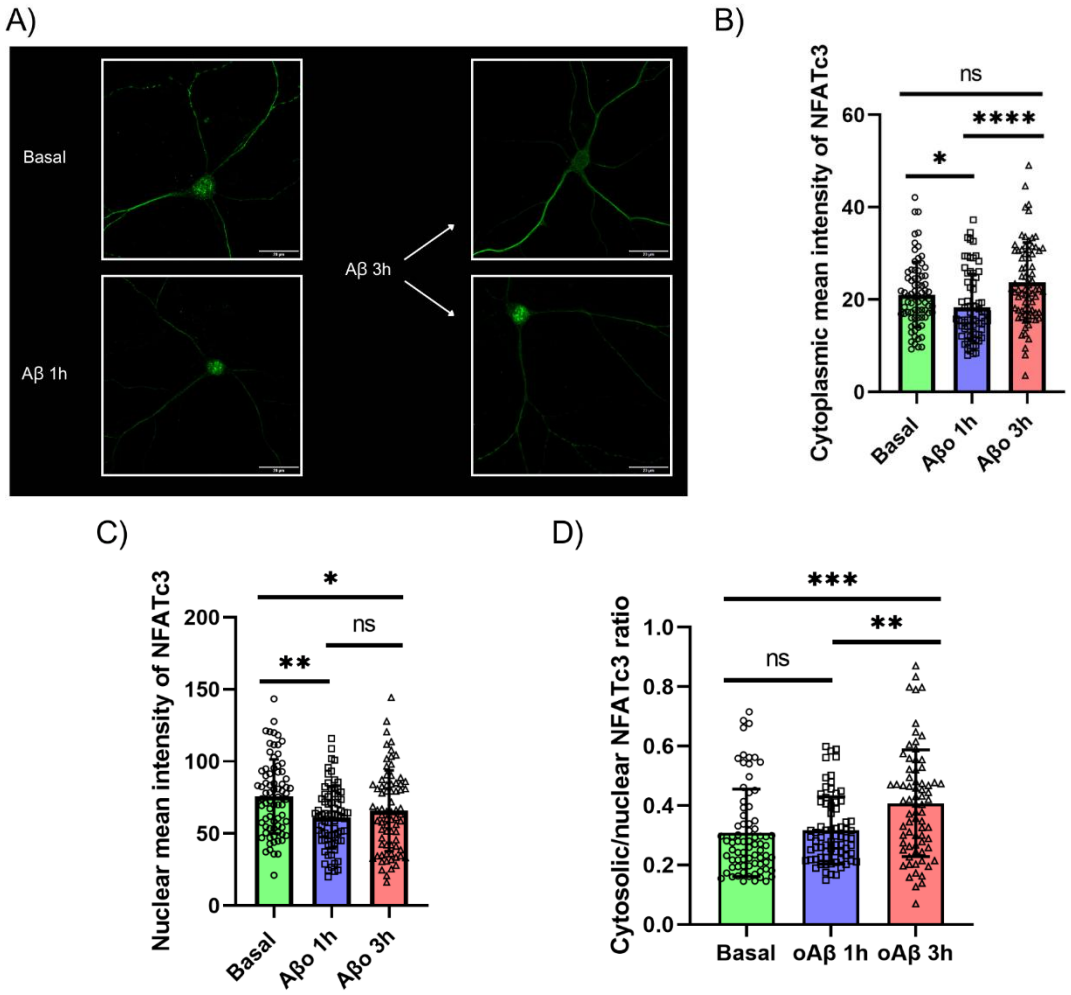

Figure 11. Aβ oligomers alter NFATc3 nuclear translocation in hippocampal neurons, despite heterogeneous responses. A) Representative images of NFATc3-stained hippocampal neurons under basal conditions or treated with Aβo for 1 hour or 3 hours using ImageJ software. After 3 hours, neurons showed heterogeneous response, with NFATc3 located on the cytoplasm (upper neuron) or the nucleus (lower neuron) depending on the cell. Scale bar: 20μm. B) Quantification of cytoplasmic mean intensity of NFATc3. C) Quantification of nuclear mean intensity of NFATc3 D) Quantification of the fluorescence intensity ratio of cytosolic/nuclear NFATc3. Data represent mean ± SD (n≈74 neurons/group from 4 independent cultures). *p<0.05, **p<0.01, ***p<0.001. Statistical analysis was determined by Kruskal-Wallis test followed by Dunn's multiple comparisons test.

5. Aβo effect on phosphorylated NFATc3

Since previous studies have documented that NFATc3 needs to be dephosphorylated by calcineurin to translocate to the nucleus (20), and because our data did not show clear nuclear translocation, we investigated the impact of amyloid-beta oligomers on the phosphorylation levels of the transcription factor. A Western-blot analysis was performed on cultured hippocampal neurons. Cells were treated with oligomers for either 1 hour or 3 hours (see materials and methods section 3.1) and neurons maintained in basal conditions (untreated) were used as control. Representative blots of pNFATc3 (upper blot) and GAPDH (lower blot) show protein levels across treatments (Figure 12A).

Even though quantification of pNFATc3 protein levels did not reveal statistically significant differences between treatments, a clear visual increase can be seen in the Aβo-treated 1 hour group in comparison with both basal and 3-hour groups (Figure 12B). These results are consistent with the dynamic NFATc3 activity in exposure to Aβo seen in previous analyses.

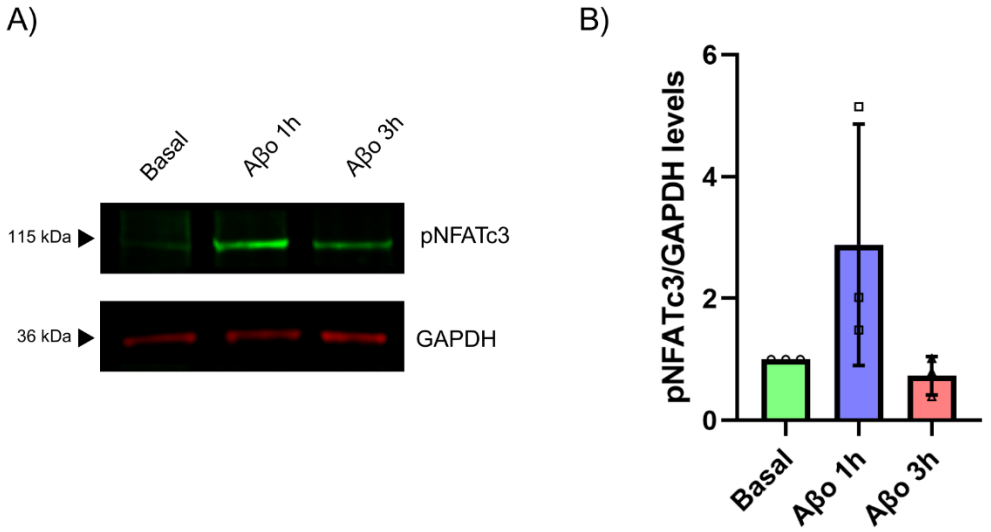

Figure 12. Aβ oligomers modulate pNFATc3 levels in hippocampal neurons. A) Representative blots showing pNFATc3 levels (upper blot) and GAPDH protein levels (lower blot) in neurons under basal conditions or treated with Aβo for 1 hour or 3 hours. B) Quantification of the pNFATc3/GAPDH ratio. Data represent mean ± SD (n=3). Statistical analysis was determined by one-way ANOVA followed by Tukey's post hoc test.

DISCUSSION

In the last years, evidence has shown that soluble oligomers of amyloid-beta are key elements in the synaptic and molecular dysfunction that characterizes the early stages (or preclinical stages) of Alzheimer's disease (31). Aβo are highly neurotoxic and capable of inducing functional alterations even before clinical symptoms appear. This early toxicity is associated with changes in synaptic plasticity, cytoskeletal reorganization and activation of signalling pathways that trigger degenerative processes (31). Understanding the cellular and molecular mechanisms through which Aβo alter neuronal functions is an essential step towards learning about the

physiopathological bases of the disease and finding more specific and effective therapeutical strategies.

Different synaptic components and signalling pathways have been described to be altered by soluble Aβ oligomers. In this regard, the AKAP79/150-CaN-NFAT complex rises as an important regulatory complex affected by Aβo in early stages of the disease (23). Previous studies have shown an Aβo-dependent decrease in AKAP150 scaffold protein expression, which alters AMPAR phosphorylation and destabilizes synaptic plasticity (23). On the other hand, it has been proposed that CaN-activated NFATc3 transcription factor suffers an anomalous nuclear translocation in presence of Aβo due to hyperactivation of CaN, favouring degenerative gene expression (24). Furthermore, although LTCCs are not directly modulated by Aβo, due to their influence on intracellular calcium dynamics, they may be able to affect Aβo-induced synaptic changes, as they have a direct anchoring to AKAP79/150 protein and regulate calcium influx that activates CaN (20).

1. Alterations in AKAP150 induced by Aβo

In previous experiments from our laboratory, a decrease in AKAP150 expression was observed after Aβo exposure. In this study, we have not only corroborated this hypothesis, but also expanded it, proving a time-dependent reduction of AKAP150 in exposure to Aβo (Figure 7). Even though the mechanism of action of this effect was not addressed in this investigation, a preceding article showed that chemically induced LTD (cLTD) decreases AKAP150 levels through the ubiquitin-proteasome system (23). Considering that Aβo is proposed to induce a pathological LTD (16), we could suggest that Aβo promote AKAP150 degradation through the ubiquitin-proteasome system.

2. Role of L-type calcium channels

Furthermore, in this study we also explored whether L-type calcium channels were involved on the Aβo-induced degradation of AKAP150 given that the scaffolding protein directly interacts with these channels (18). We analysed the levels of AKAP150 after blocking the channels with nimodipine in exposure to the oligomers. Even though results were not statistically significant, we observed a similar decrease in AKAP150 expression in 1-hour Aβo treatment and in Aβo + nimodipine group, while nimodipine-only group showed an increase in protein levels (Figure 8). These data suggest that, at least in the context of AKAP150, L-type calcium channels are not involved in its Aβo-induced reduction.

However, we cannot rule out the effect of LTCCs in the AKAP-CaN-NFAT signalling pathway affected by Aβo. In this regard, studies state that LTCCs contribute to dendritic excitability and gene-expression regulation (18). Considering that it has been demonstrated that L-channels directly interact with and are regulated by AKAP79/150, which modulates CaN and subsequently activates NFATc3 transcription factor (20), LTCCs play a major role in the regulation of this pathway. Further experiments could analyse the impact of blocking LTCCs on CaN activity or NFATc3 localization in presence of Aβo.

3. Changes in PSD-95 and synaptic plasticity

On the other hand, to evaluate the synaptic state of neurons, we analysed the presence of PSD-95 anchoring protein as a synaptic marker in dendrites after exposure to Aβo. Previous studies have shown that cLTD trigger a decrease in PSD-95 puncta in neurons, which is related to synaptic dysfunction (24). Furthermore, it has been described that Aβo are able to induce a reduction in PSD-95 levels through CaMKII-dependent mechanisms (22).

In our study, we observed a significant decrease in PSD-95 spots after 1-hour treatment, which correlates with that seen in synaptic loss. Nevertheless, at 3-hour treatment, spots significantly increased compared to 1 hour treatment. Compared to basal, non-significant differences were observed in the 3-hour treatment, reaching non-treated levels, although high variability was detected (Figure 9).

These results could be interpreted as a compensatory mechanism from neurons. In an initial phase (1 hour), acute exposition of Aβo induces a rapid loss of PSD-95. However, after a recovery phase (3 hours), neurons could activate plasticity compensatory mechanisms trying to restore initial synaptic functions by augmenting PSD-95 expression. This type of response has been described in the entorhinal cortex of AD patients, with an increase of PSD-95 immunoreactivity in this region (32). Moreover, some articles have also highlighted the existence of a dynamic regulation of PSD-95 in early stages of AD, inducing homeostatic mechanisms (33). Due to this, our results suggest a compensatory plasticity of PSD-95 protein caused by Aβo.

4. Location and regulation of NFATc3

In this part of the investigation, firstly we analysed the dendritic localization of NFATc3 after exposure to Aβo for 1 hour and 3 hours. We quantified 3 parameters (occupied area, volume and mean fluorescent intensity of dendritic NFATc3), and in the three of them similar patterns were observed: a significant decrease in the 1-hour group and an increase in the 3-hour group that does not reach basal levels but is significant towards the 1-hour group (Figure 10). NFATc3 dendritic localization has not been specifically described in literature, even though it has been documented that NFATc3 translocates to the nucleus after Aβo exposure (24). This event occurs mainly due to the interaction of Aβo with NMDARs, and due to an increase in calcium influx by LTCCs which activates CaN and dephosphorylates the transcription factor. The latter pathway may be especially affected by the loss of AKAP150 as mentioned before, as this anchoring protein regulates the function of LTCCs.

The results we obtained after 1 hour of Aβo concur with this hypothesis, showing a reduction in dendritic NFATc3 likely due to nuclear translocation. However, after 3 hours of Aβo exposure, the signal increases in dendrites. This result contrasts previous articles that discuss a sustained nuclear translocation even with 3 hours of Aβo treatment (24). A possible explanation for this discrepancy could be a difference in treatment protocols. Previous studies used a final concentration of 500nM of Aβo in neurons, maintaining it for the whole experiment (24). Our treatment, however,

consisted of exposure to 5 μM of Aβo for 10 minutes, followed by replacement and incubation with ACSF (specified in materials and methods section 3.1). Considering that NFATc3 is a transcription factor, is possible that, without consistent exposure to Aβo, after the activation of target genes in the nucleus it returns to the cytoplasm once it has done its function.

Moreover, we observed high variability in the basal group values, which could be due to heterogeneity of cultures, such as cortical tissue and glial cells reducing culture purity and inclusion of different neuronal types (excitatory or inhibitory) during image obtaining.

To deepen the investigation about NFATc3 dynamics in response to Aβo, we analysed the cellular distribution by evaluating cytoplasmic and nuclear mean fluorescence intensities, as well as the cytoplasmic/nuclear ratio. Under basal conditions and after 1 hour of Aβo treatment similar conditions were observed. However, after 3-hour treatment, we observed major heterogeneity in NFATc3 localization. Some neurons showed clear nuclear translocation, while others maintained the transcription factor in the cytoplasm.

Our results showed that cytoplasmic mean intensity of NFATc3 decreased significatively after 1 hour of treatment but subsequently increased after 3 hours. Regarding nuclear signal, a significant decrease was observed in both 1-hour and 3-hour treatments comparing to basal. Moreover, the cytoplasmic/nuclear ratio showed a statistically significant increase at 3-hour treatment with Aβo (Figure 11).

Cytoplasmic decrease and subsequent increase in NFATc3 align with the results obtained in dendritic NFATc3 signal. We could discuss that the transcription factor is on the way to enter the nucleus at the 1-hour mark and then goes back to the cytoplasm once it has finished nuclear induction of genes. The cytoplasmatic/nuclear ratio increase we observed in the 3-hour group also supports this idea.

To explain the decrease in the nuclear mean intensity levels of Aβo-groups, however, we could argue that the lack of nuclear translocation could be due to the loss of AKAP150 expression by Aβo treatment. As mentioned before, AKAP150 anchors CaN near substrates for dephosphorylation, and Aβo decreases the levels of the scaffolding protein (23). This could impede the whole regulation of NFAT dephosphorylation, and thus, its nuclear translocation.

Supporting this last hypothesis, our results in phosphorylated NFATc3 (Figure 12) showed a visual, though not statistically significant increase of the group treated with 1 hour of Aβo. This suggests that NFATc3 remained phosphorylated and that CaN did not dephosphorylate it, maybe due to the lack of AKAP150 to anchor it close to the substrate, obstructing its entrance to the nucleus.

Both hypothesis (nuclear translocation of NFATc3 and subsequent exit to the cytoplasm; NFATc3 dysregulation due to the lack of AKAP150) are not mutually exclusive but could coexist in different neuronal subtypes and in different phases of Aβo exposure. Further experiments are needed to establish the behaviour of NFATc3 in neurons, such as the analysis of NFATc3-activated degenerative genes

such as Mdm2, which could give information about the effective nuclear translocation of the transcription factor. Moreover, silencing of AKAP150 via shRNA (shAKAP150) could give us more information about the AKAP150-CaN-NFAT complex and the changes in NFATc3 location. This hindsight could help evaluate whether AKAP150 alters NFATc3 nuclear translocation and, thus, its function as transcription factor.

In summary, our study provides new insights about the early synaptic dysfunction caused by amyloid-beta oligomers via the AKAP150-CaN-NFAT complex and suggests a time-dependent dynamic regulation of these proteins in exposure to Aβo. Understanding these molecular processes is essential for the development of more specific and effective therapeutical strategies against Alzheimer's disease. Even though additional studies are needed to untangle the molecular pathways altered by Aβo, our results highlight the importance of studying early synaptic changes, as well as the possible role of L-type calcium channels in modulating these changes. Further investigation of these initial alterations could open new therapies to slow down or prevent synaptic dysfunction in AD.

CONCLUSION

The data obtained in this study supports the hypothesis that Aβ oligomers alter the AKAP150-CaN-NFAT signalling pathway in neurons, with AKAP150 being a key element in maintaining the integrity of the intracellular calcium signalling. Its loss contributes to the dysregulation of NFATc3, which could represent one of the molecular mechanisms involved in synaptic dysfunction on early stages of Alzheimer's disease.

REFERENCES

1. World Health Organization [Internet]. [cited 2025 Jun 30]. Dementia. Available from: https://www.who.int/en/news-room/fact-sheets/detail/dementia
2. 2025 Alzheimer's disease facts and figures. Alzheimer's & Dementia [Internet]. 2025 Apr 29;21(4). Available from: https://alz-journals.onlinelibrary.wiley.com/doi/10.1002/alz.70235
3. Abdul Manap AS, Almadodi R, Sultana S, Sebastian MG, Kavani KS, Lyenouq VE, et al. Alzheimer's disease: a review on the current trends of the effective diagnosis and therapeutics. Vol. 16, Frontiers in Aging Neuroscience. Frontiers Media SA; 2024.
4. Zheng Q, Wang X. Alzheimer's disease: insights into pathology, molecular mechanisms, and therapy. Protein Cell. 2024 Feb 1;
5. Cline EN, Bicca MA, Viola KL, Klein WL. The Amyloid-β Oligomer Hypothesis: Beginning of the Third Decade. Vol. 64, Journal of Alzheimer's Disease. IOS Press; 2018. p. S567–610.
6. El Abiad E, Al-Kuwari A, Al-Aani U, Al Jaidah Y, Chaari A. Navigating the Alzheimer's Biomarker Landscape: A Comprehensive Analysis of Fluid-Based Diagnostics. Vol. 13, Cells. Multidisciplinary Digital Publishing Institute (MDPI); 2024.
7. Grande G, Valletta M, Rizzuto D, Xia X, Qiu C, Orsini N, et al. Blood-based biomarkers of Alzheimer's disease and incident dementia in the community. Nat Med. 2025 Jun 1;

8. Passeri E, Elkhoury K, Morsink M, Broersen K, Linder M, Tamayol A, et al. Alzheimer's Disease: Treatment Strategies and Their Limitations. Vol. 23, International Journal of Molecular Sciences. MDPI; 2022.
9. Wu CK, Fuh JL. A 2025 update on treatment strategies for the Alzheimer's disease spectrum. Journal of the Chinese Medical Association. Wolters Kluwer Health; 2025.
10. Zhang J, Zhang Y, Wang J, Xia Y, Zhang J, Chen L. Recent advances in Alzheimer's disease: Mechanisms, clinical trials and new drug development strategies. Vol. 9, Signal Transduction and Targeted Therapy. Springer Nature; 2024.
11. Sanderson JL, Dell'Acqua ML. AKAP signaling complexes in regulation of excitatory synaptic plasticity. Vol. 17, Neuroscientist. 2011. p. 321–36.
12. Jurado S. AMPA receptor trafficking in natural and pathological aging. Vol. 10, Frontiers in Molecular Neuroscience. Frontiers Media S.A.; 2018.
13. Sumi T, Harada K. Mechanism underlying hippocampal long-term potentiation and depression based on competition between endocytosis and exocytosis of AMPA receptors. Sci Rep. 2020 Dec 1;10(1).
14. Prikhodko O, Freund RK, Sullivan E, Kennedy MJ, Dell'Acqua ML. Amyloid-β causes NMDA receptor dysfunction and dendritic spine loss through mGluR1 and AKAP150-anchored calcineurin signaling. The Journal of Neuroscience. 2024 Sep 11;e0675242024.
15. Hampel H, Hardy J, Blennow K, Chen C, Perry G, Kim SH, et al. The Amyloid-β Pathway in Alzheimer's Disease. Vol. 26, Molecular Psychiatry. Springer Nature; 2021. p. 5481–503.
16. Zhang H, Jiang X, Ma L, Wei W, Li Z, Chang S, et al. Role of Aβ in Alzheimer's-related synaptic dysfunction. Vol. 10, Frontiers in Cell and Developmental Biology. Frontiers Media S.A.; 2022.
17. Raïch I, Lillo J, Rebassa JB, Capó T, Cordomí A, Reyes-Resina I, et al. Dual Role of NMDAR Containing NR2A and NR2B Subunits in Alzheimer's Disease. Int J Mol Sci. 2024 May 1;25(9).
18. Oliveria SF, Dell'Acqua ML, Sather WA. AKAP79/150 Anchoring of Calcineurin Controls Neuronal L-Type Ca2+ Channel Activity and Nuclear Signaling. Neuron. 2007 Jul 19;55(2):261–75.
19. Wild AR, Dell'Acqua ML. Potential for therapeutic targeting of AKAP signaling complexes in nervous system disorders. Vol. 185, Pharmacology and Therapeutics. Elsevier Inc.; 2018. p. 99–121.
20. Murphy JG, Crosby KC, Dittmer PJ, Sather WA, Dell'Acqua ML. AKAP79/150 recruits the transcription factor NFAT to regulate signaling to the nucleus by neuronal L-type Ca2+ channels. Mol Biol Cell. 2019 Jul 1;30(14):1743–56.
21. Chen X, Crosby KC, Feng A, Purkey AM, Aronova MA, Winters CA, et al. Palmitoylation of A-kinase anchoring protein 79/150 modulates its nanoscale organization, trafficking, and mobility in postsynaptic spines. Front Synaptic Neurosci. 2022 Sep 15;14.
22. Proctor DT, Coulson EJ, Dodd PR. Post-synaptic scaffolding protein interactions with glutamate receptors in synaptic dysfunction and Alzheimer's disease. Vol. 93, Progress in Neurobiology. 2011. p. 509–21.
23. Cheng W, Siedlecki-Wullich D, Català-Solsona J, Fábregas C, Fadó R, Casals N, et al. Proteasomal-mediated degradation of akap150 accompanies ampar endocytosis during cltd. eNeuro. 2020 Mar 1;7(2).

24. Woolfrey KM, Dell'acqua ML, Martinez TP, Larsen ME, Sullivan E. Amyloid-β-Induced Dendritic Spine Elimination Requires Ca2+-Permeable AMPA Receptors, AKAP-Calcineurin-NFAT Signaling, and the NFAT Target Gene Mdm2. eNeuro. 2024 Mar 1;11(3).
25. Chowdhury MAR, Haq MM, Lee JH, Jeong S. Multi-faceted regulation of CREB family transcription factors. Vol. 17, Frontiers in Molecular Neuroscience. Frontiers Media SA; 2024.
26. Solsona JC. Role of Nr4a2 transcription factor in hippocampal synaptic plasticity. Possible therapeutic target for Alzheimer's disease.
27. Müller MR, Rao A. NFAT, immunity and cancer: A transcription factor comes of age. Vol. 10, Nature Reviews Immunology. 2010. p. 645–56.
28. Mackiewicz J, Lisek M, Boczek T. Targeting CaN/NFAT in Alzheimer's brain degeneration. Vol. 14, Frontiers in Immunology. Frontiers Media SA; 2023.
29. Chen F, Chu CC, Wu CY, Chen F, Xu J, Zhou L, et al. Targeting AKAP79/150 in Human Disorders: An Emerging Opportunity for Future Therapies? Prog Neurobiol. 2023 Jul 31;1–18.
30. Fa M, Orozco IJ, Francis YI, Saeed F, Gong Y, Arancio O. Preparation of oligomeric β-amyloid1-42 and induction of synaptic plasticity impairment on hippocampal slices. Journal of Visualized Experiments. 2010 Jul;(41).
31. Tang H, Andrikopoulos N, Li Y, Ke S, Sun Y, Ding F, et al. Emerging biophysical origins and pathogenic implications of amyloid oligomers. Nature Communications . 2025 Dec 1;16(1).
32. Leuba G, Walzer C, Vernay A, Carnal B, Kraftsik R, Piotton F, et al. Postsynaptic density protein PSD-95 expression in Alzheimer's disease and okadaic acid induced neuritic retraction. Neurobiol Dis. 2008 Jun;30(3):408–19.
33. Savioz A, Leuba G, Vallet PG. A framework to understand the variations of PSD-95 expression in brain aging and in Alzheimer's disease. Vol. 18, Ageing Research Reviews. Elsevier Ireland Ltd; 2014. p. 86–94.